

Supporting Information

Fluorinated Graphene: A Promising Macroscale Solid Lubricant under Various Environments

Yanfei Liu, Jinjin Li, Xinchun Chen, Jianbin Luo*

State Key Laboratory of Tribology, Tsinghua University, Beijing 100084, China

Corresponding author:

*To whom all correspondence should be addressed.

Jinjin Li

Telephone: 8610-62789482

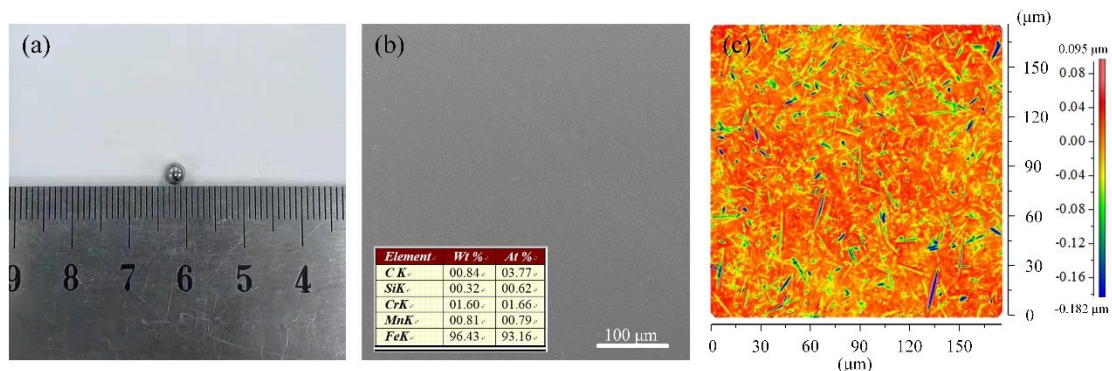


Figure S1. (a) Picture of the original steel counterpart ball. (b) Surface morphology of the original steel ball obtained with scanning electron microscopy, where the inset is the chemical composition. (c) Surface morphology of the original steel ball obtained with 3D white-light interferometer.

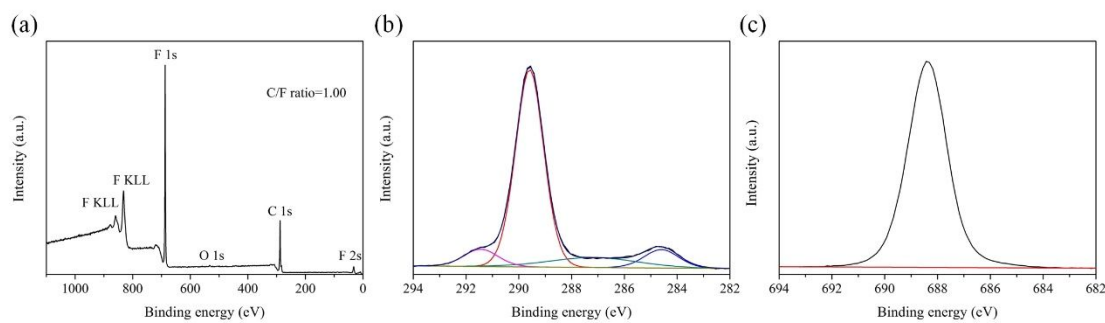


Figure S2. (a) The full XPS spectrum of the original FG nanoflakes. (b, c) The XPS spectra of C 1s and F 1s of the original FG nanoflakes. The C/F ratio of FG nanoflakes is 1.00.

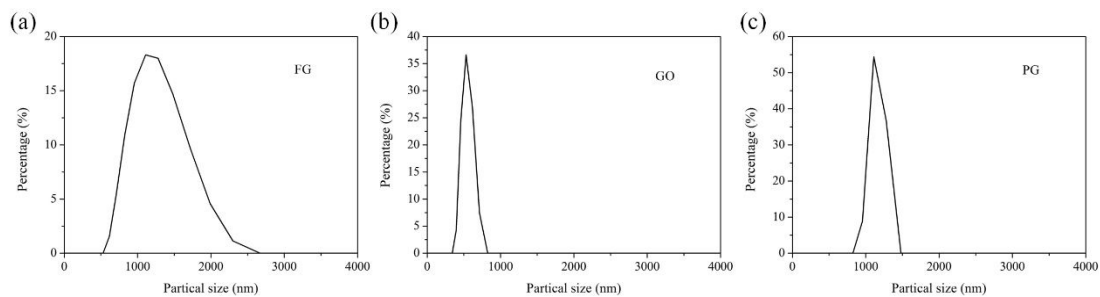


Figure S3. The size distribution of (a) FG, (b) GO and (c) pristine graphene nanoflakes.

The average particle size of FG, GO and pristine graphene nanoflakes were 1223 μm , 782 μm and 1278 μm , respectively.

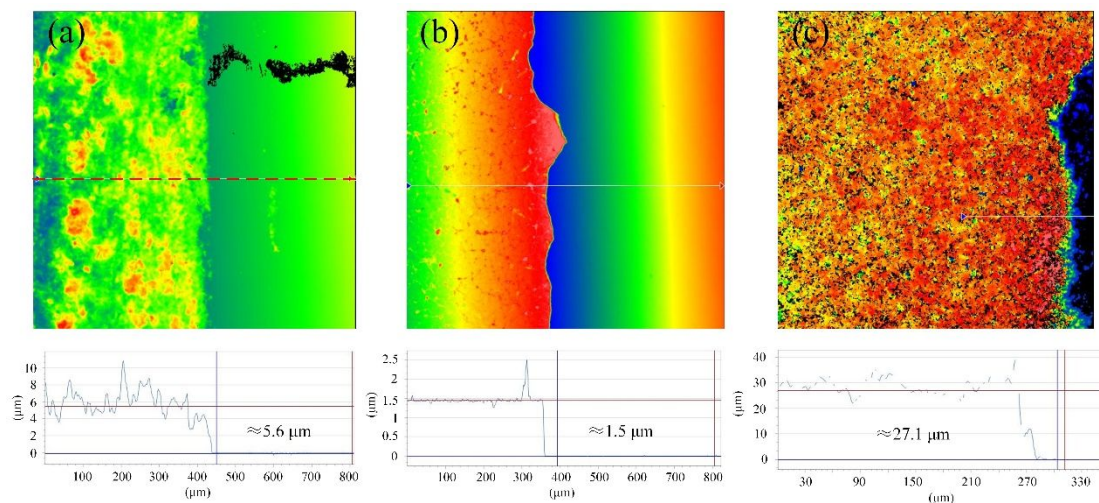


Figure S4. The thickness of the (a) FG coating, (b) GO coating and (c) pristine graphene coating.

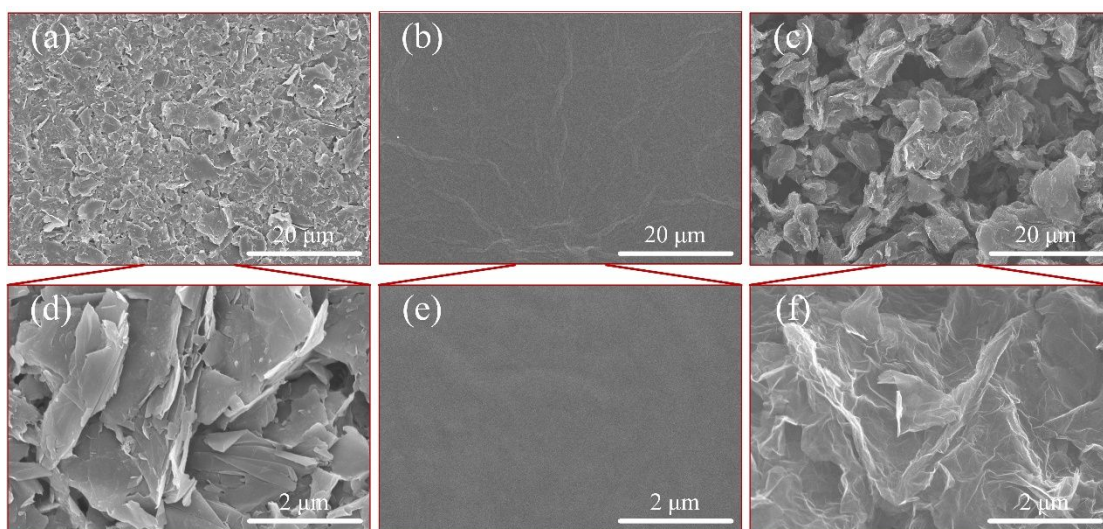


Figure S5. The scanning electron microscopy image of the original (a, d) FG coating, (b, e) GO coating and (c, f) pristine graphene coating.

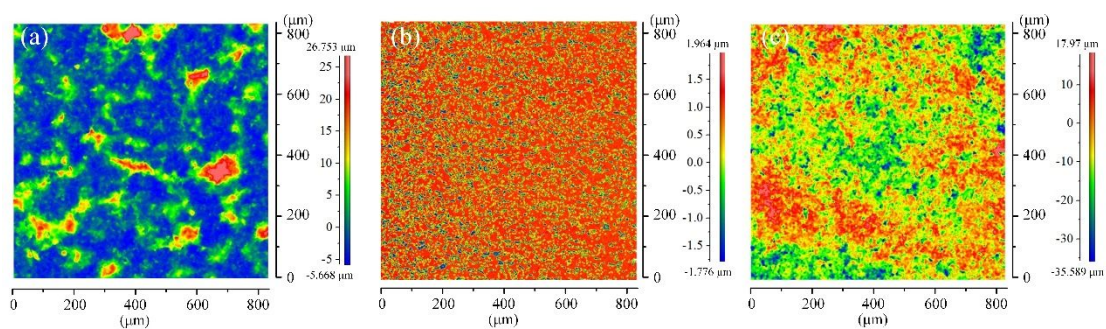


Figure S6. The 3D white-light interferometer image of the original (a) FG coating, (b) GO coating and (c) pristine graphene coating.

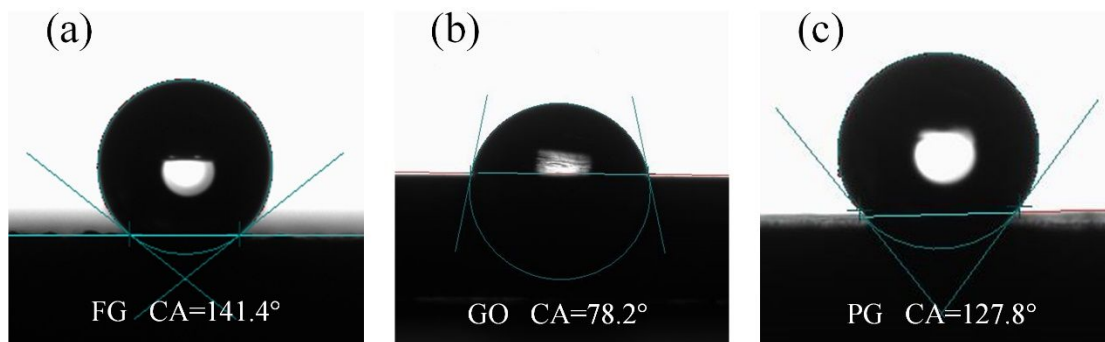


Figure S7. The contact angle of (a) FG coating, (b) GO coating and (c) pristine graphene coating were 141.4°, 78.2° and 127.8°, respectively.

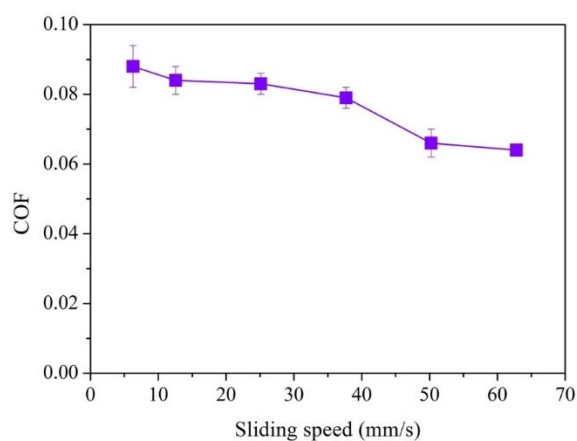


Figure S8. Average stable state COF with different sliding speeds (3N, 45% RH, with FG coating).

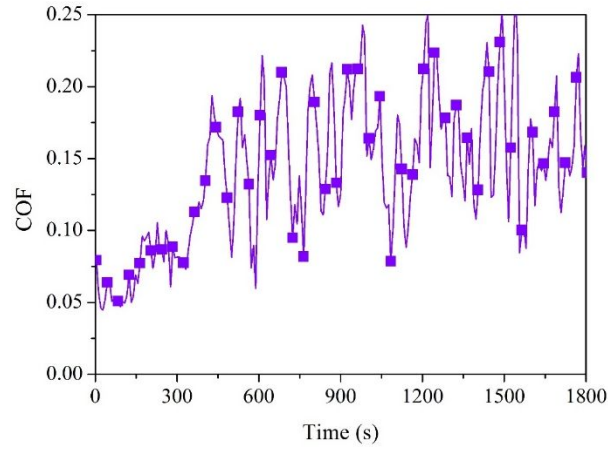


Figure S9. COF as a function of the time with the normal load of 3 N for the SS substrate with FG coating under 70% RH.

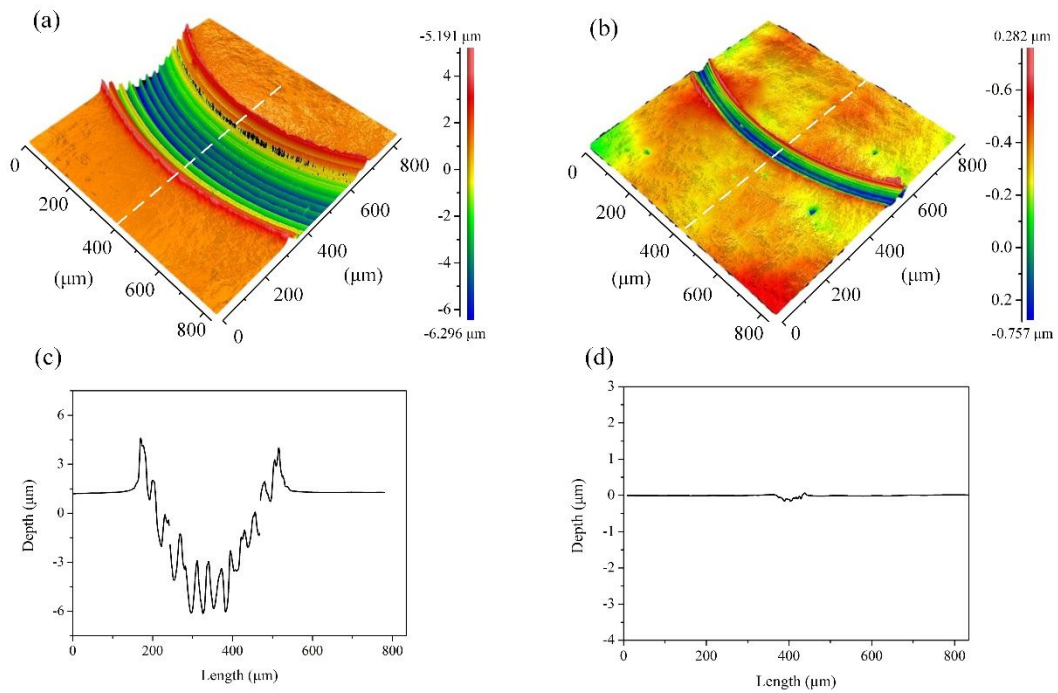


Figure S10. Wear scar morphology after the 30-min friction test at the normal load of 3 N under the air atmosphere with the RH of 10%. 3D morphologies and 2D line profiles of the wear tracks of the (a, c) bare SS substrate and (b, d) SS substrate deposited with the FG coating, respectively.

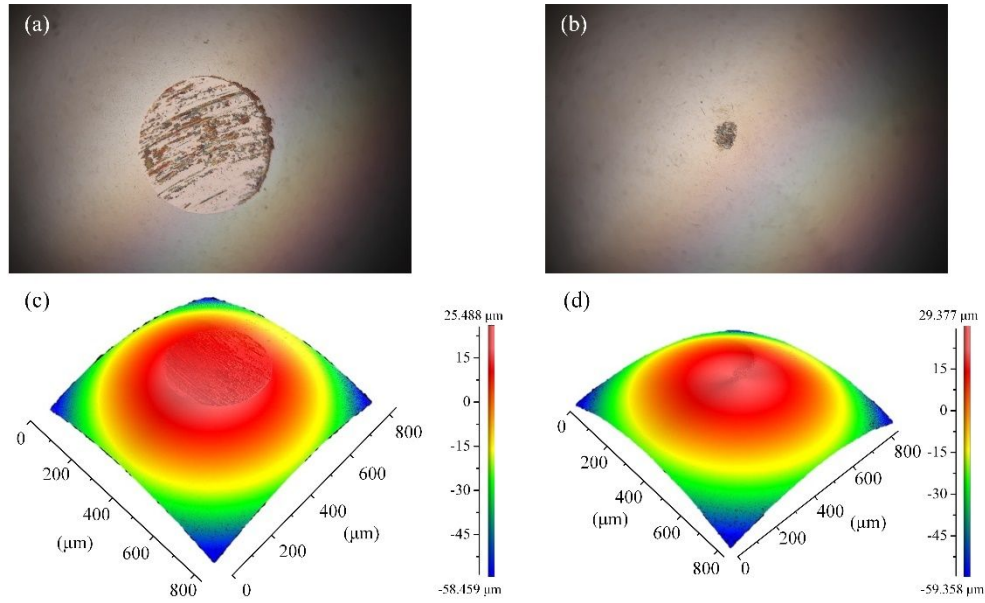


Figure S11. Wear scar morphology of the steel counterpart ball after the 30-min friction under the normal load of 3 N (RH: 10%). Photographs and 3D morphologies of the steel counterpart balls sliding against the (a, c) bare SS substrate and (b, d) SS substrate with the FG coating, respectively.

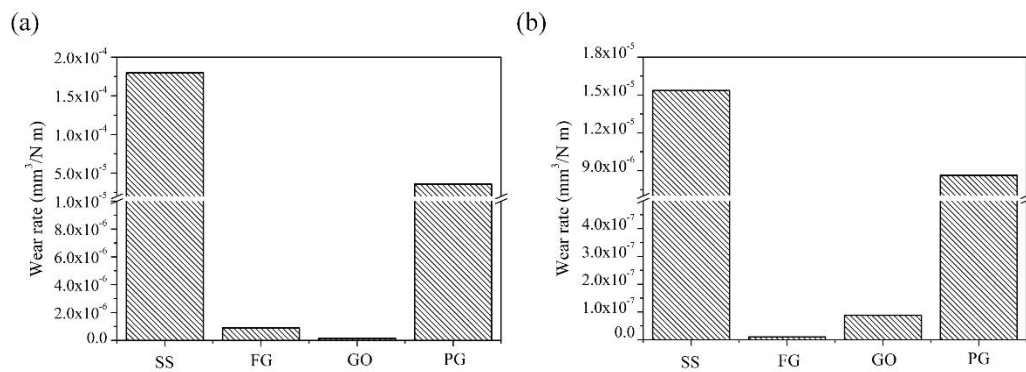


Figure S12. Wear rate of the (a) SS substrates and the (b) steel counterpart balls after the 30-min friction (3 N, 10% RH) with different coatings

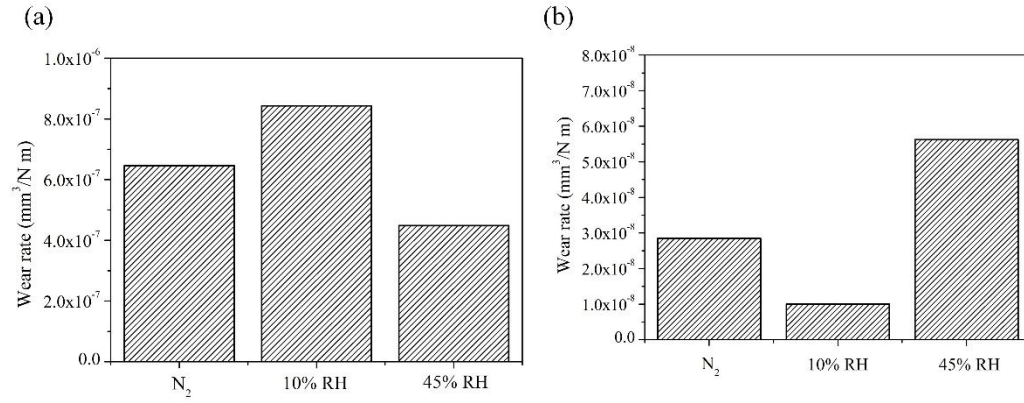


Figure S13. Wear rate of the (a) SS substrates and the (b) steel counterpart balls after the 30-min friction (3 N) under different atmospheres with FG coating.

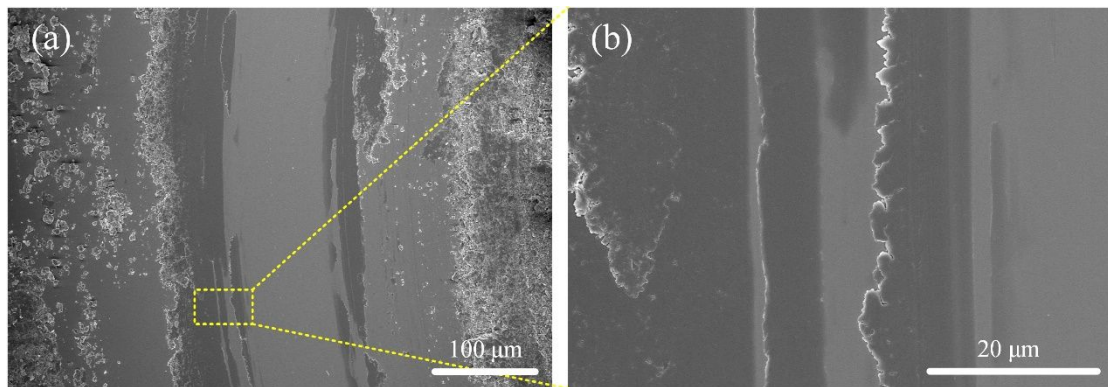


Figure S14. (a) SEM image of the wear track on the SS substrate deposited with the FG coating after the 30-min friction test (1 N, 10%) and (b) the enlarged SEM image of the thick tribofilm in the wear track.

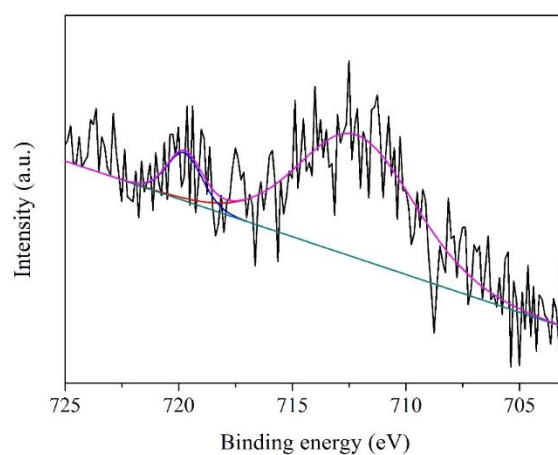


Figure S15. XPS spectrum of Fe 2p on the wear track of SS substrate deposited with the FG coating at the normal load of 1 N under the air atmospheres with the RH of 10%.

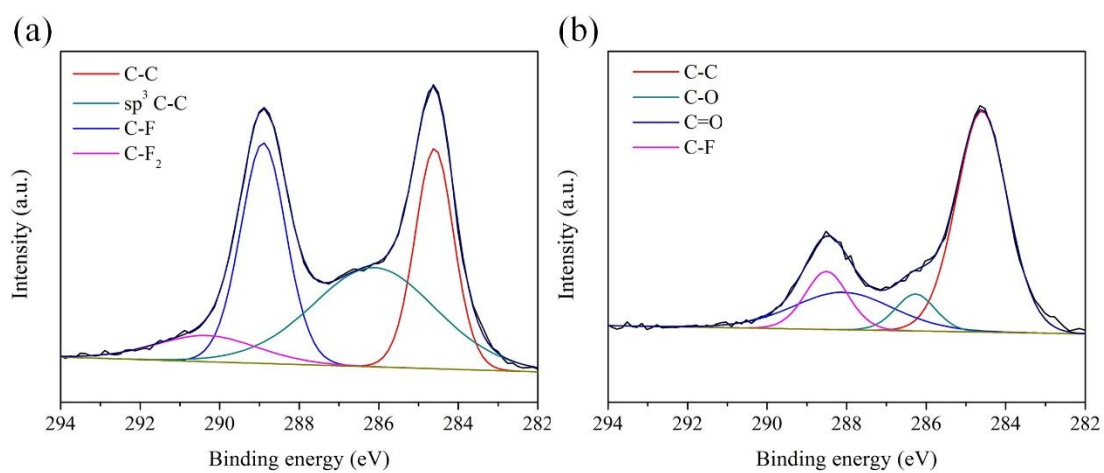


Figure S16. XPS spectra of the wear track on SS substrate deposited with the FG coating at the normal load of 3 N under the (a) N_2 , (b) air atmospheres with the RH of 30%.

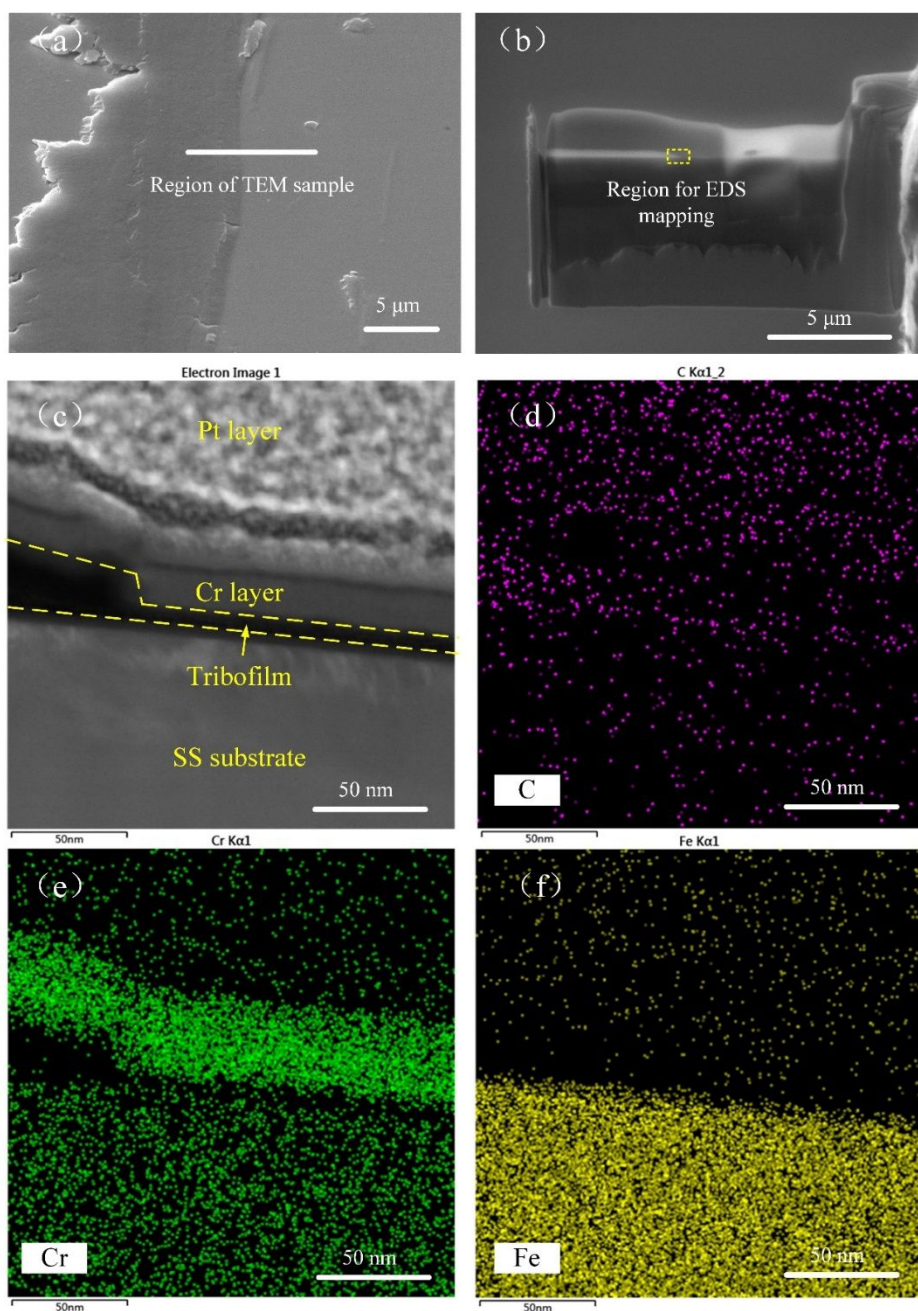


Figure S17. (a) Location of the TEM sample. (b) SEM image of the TEM sample prepared with FIB. (c) Low resolution TEM image on the boundary between the thick tribofilm and the thin tribofilm. (d-f) EDS mapping results for C, Cr and Fe, respectively.

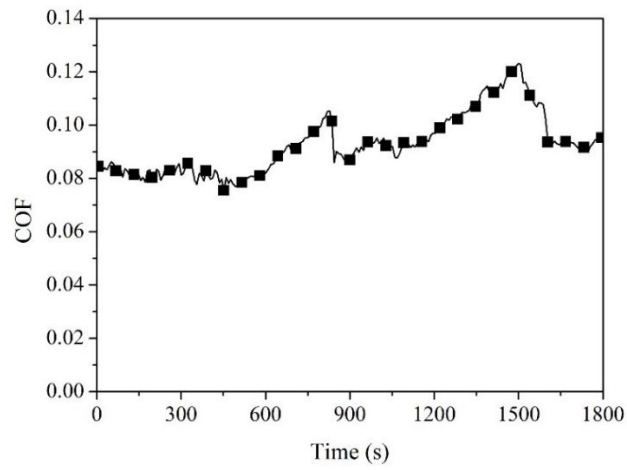


Figure S18. COF as a function of the time under the normal load of 3 N for the SS substrate with drop casted FG coating.

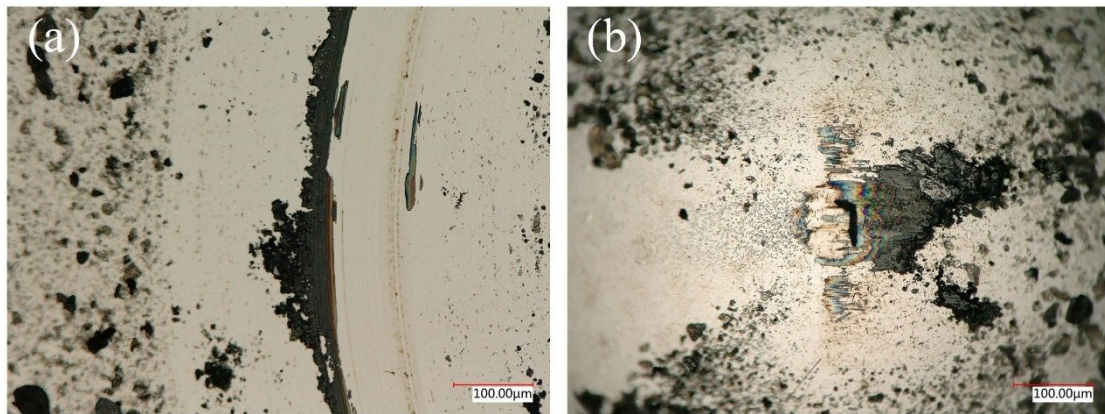


Figure S19. The wear scar morphology of the (a) SS substrate with drop casted FG coating and (b) the steel counterpart ball after the 30-min friction test with 3N normal load.

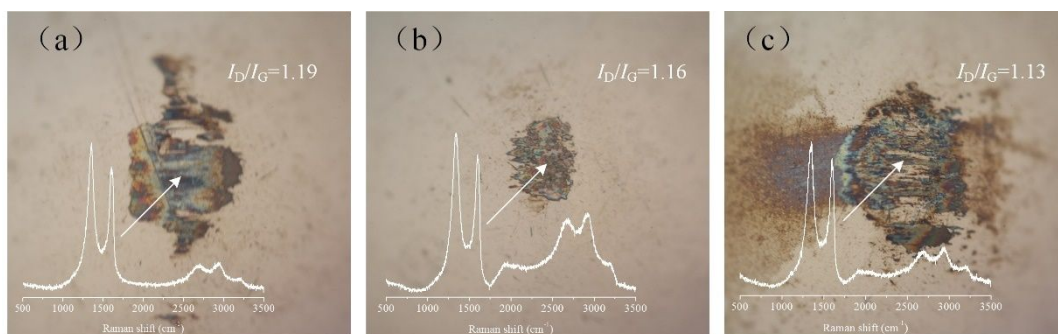


Figure S20. Surface morphologies of the steel counterpart balls sliding against the SS substrate deposited with the FG coating at the normal load of 3 N under the (a) nitrogen and air atmospheres with the RHs of (b) 10% and (c) 45%.

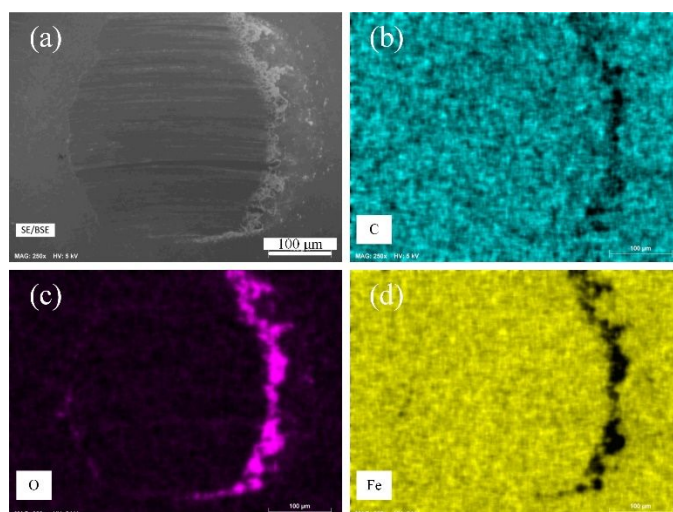


Figure S21. Analysis of the wear scar on the steel counterpart ball after the 30-min friction test (3 N, RH: 10%) against the SS substrate deposited with the pristine graphene coating. (a) SEM image of the wear scar, (b–d) EDS elemental maps of C, O and Fe, respectively.

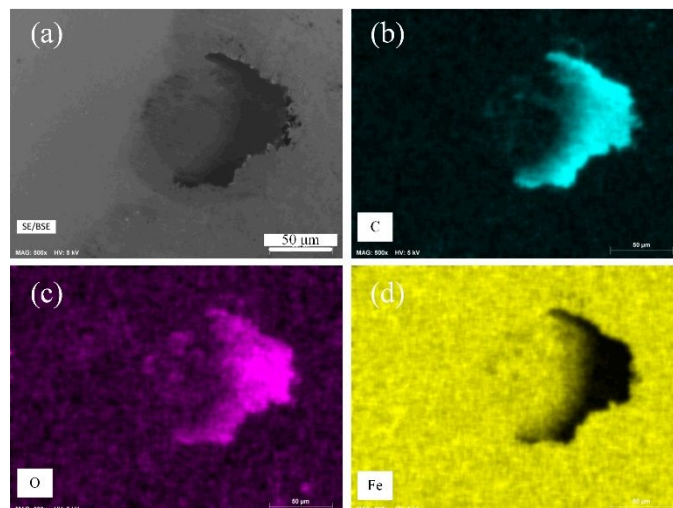


Figure S22. Analysis of the wear scar on the steel counterpart ball after the 30-min friction test (3 N, RH: 10%) against the SS substrate deposited with the GO coating. (a) SEM image of the wear scar, (b–d) EDS elemental maps of C, O and Fe, respectively.

Table 1. Comparison of System Energy Corrugation ($E_{\max} - E_{\min}$) and Shear Strength, τ , for the Graphene, GO and FG Systems.

Material	Energy corrugation $E_{\max} - E_{\min}$	Shear strength τ (GPa)	Ref.
Graphene	1.41	0.33	[S1]
GO	4.19-22.17	0.46-4.48	[S2]
FG	0.34	0.124	[S1]

References

- [S1] Wang, L.-F.; Ma, T.-B.; Hu, Y.-Z.; Wang, H.; Shao, T.-M., Ab Initio Study of the Friction Mechanism of Fluorographene and Graphane. *J Phys. Chem. C* **2013**, *117* (24), 12520-12525.
- [S2] Wang, L.-F.; Ma, T.-B.; Hu, Y.-Z.; Wang, H., Atomic-scale friction in graphene oxide: An interfacial interaction perspective from first-principles calculations. *Phys. Rev. B* **2012**, *86* (12), 125436.